JTTEE5 13:265-273
DOI: 10.1361/10599630419418
1059-9630/$19.00 © ASM International

Analysis of Tantalum Coatings Produced by the Kinetic Spray Process

T. Van Steenkiste and D.W. Gorkiewicz

(Submitted 2 April 2003; in revised form 22 May 2003)

Tantalum (Ta) coatings have been produced using a relatively new process, kinetic spray. Ta starting powders having particle diameters greater than 65 μm are injected into a de Laval-type nozzle, entrained in a supersonic gas stream, and accelerated to high velocities due to drag effects. The particles' kinetic energy is transformed via plastic deformation into strain and heat on impact with the substrate surface. Particles are not thermally softened or melted, producing relatively low oxide, reduced residual stress, high adhesion and low porosity coatings. Analysis of the mechanical and physical properties of these Ta coatings demonstrated increasing hardness, cohesive adhesion, and decreasing porosity as a function of particle velocity. Comparison between kinetically sprayed coatings and coatings produced using conventional coating methods will be discussed.

Keywords coatings, cold spray, kinetic spray, tantalum

1. Introduction

Tantalum (Ta) is an element that possesses excellent corrosion resistance, good formability, a high melting point (2996 °C), a low coefficient of expansion, excellent wear resistance, and high density with a strength-to-weight ratio almost 2.5 times higher than steel. Ta coatings are resistant to nitric acid, phosphoric acid, acetic acid, hydrochloric acid, sulphuric acid, bromine, hydrogen peroxide, chlorine, etc. These physical properties make TA coatings attractive to the petrochemical and metallurgical industries.[3-5] However, Ta is also very reactive and usually cannot be used above 500 °C without reacting with gases such as O_2, H_2, N_2, and CO_2. The resulting oxidation produces a severe loss of ductility and cracking of the metal's surface. This reactivity requires that for a coating process used in the formation of Ta coatings, such as vacuum plasma spray (VPS), plasma spray (PS), high velocity oxygen-fuel (HVOF), or chemical vapor deposition (CVD), coatings must be done in a vacuum or in an inert atmosphere (shrouding or closed chamber).[3] Ta coatings can also be formed electrochemically from a molten salt or sputtered using a magnetron sputtering system.[4]

Several Ta coatings were produced in air on brass substrates without the need for an inert gas shrouding or vacuum chamber using a relatively new process known as kinetic spray. In the kinetic spray method, particles of diameter 65-200 μm in diameter are accelerated to velocities ranging from 250-450 m/s to produce coatings, having relatively low residual stress and low oxide content. The particles are not thermally softened or melted in the kinetic spray process so chemical reactions of the Ta are minimal. The kinetic and cold spray processes have been described in detail before[1,6-19]; however, a brief description of the process follows.

T. Van Steenkiste and **D.W. Gorkiewicz,** Delphi Research Laboratories, Shelby Township, MI, 48315. Contact e-mail: thomas.van.steenkiste@delphi.com.

Schematic diagrams of the kinetic spray apparatus are shown in Fig. 1. The process involves preheating the main airflow and combining it with the powder/N_2 mixture, from the high-pressure powder feeder, in a premixing chamber. The N_2 gas flowing through the powder feeder is at room temperature for all the results reported in this study. The purpose of heating the main gas is not to heat the particles (however with increasing main gas temperature there is also a corresponding increase in particle temperature[1,6,13-19]), but rather to increase the particle velocity, as discussed below. This combination of gas and particles flows through a de Laval-type nozzle and the particles accelerate due to drag effects with the high velocity gas. Down stream of the throat in the de Laval-type nozzle the gas velocity becomes supersonic. The speed of sound υ is given by

$$\nu = (\gamma RT/M_w)^{1/2} \quad \text{(Eq 1)}$$

where γ is the specific heat ratio (1.4 for air and 1.66 for He), R is the gas constant (8314 J/kmol K), T is the gas temperature, and M_w is the molecular weight of the gas. To increase the gas velocity and, ultimately, the particle velocity through drag effects, one would increase the gas temperature and/or choose a gas of lower molecular weight such as helium (He).

The conversion of the particle's kinetic energy to heat and strain energy occurs when the particles impact the substrate surface at high velocity. Subsequent particles impact previously deposited particles, deform, and bond to produce a coating of increasing thickness.[1]

2. Properties of the Kinetic Process

Coatings are produced using initial particle size distributions between 65 and 200 μm in diameter. This larger size particle distribution results in a lower particle velocity and lower threshold velocities.[1] By comparison the cold spray process uses particle diameters less than 50 μm with higher particle velocities, a higher mean critical velocity, and usually lower particle temperatures.[13-19] Since the kinetic energy scales as d^3 where d is

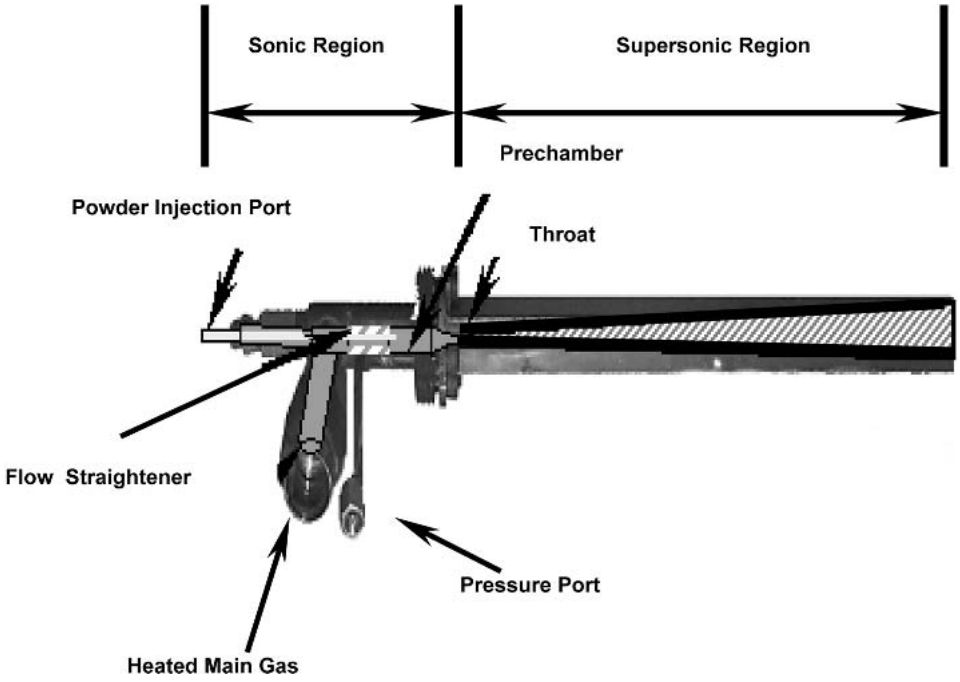

Fig. 1 Close-up diagram of the nozzle components

the particle diameter and as v^2 where v is the particle velocity, the total kinetic energy, available for plastic deformation is usually greater for the slower moving, larger diameter particles of the kinetic spray process than for the faster, smaller diameter particles of the cold spray method. Although, a larger diameter particle requires increased deformation energy, ultimately it is the yield strength of the particle that must be exceeded.[1] Presumably, this is the basis of the mean critical velocity threshold, the velocity above, which the majority of the particles start to form coatings (i.e., the point at which the total available energy equals the energy needed for plastically deformation, fracturing of surface oxide layers, etc.). Large diameter particles (greater than 65 μm) usually have a lower mean critical velocity than small diameter particles (less than 50 μm).[1]

Large diameter powder particles used in the kinetic spray process have several mechanical and economical advantages compared with smaller diameter powders. Explosibility, minimum energy for ignition, and rate of pressure rise,[20] all decrease as the particle diameter increases. Health risks decrease as powder particle sizes increases because the human body has mechanisms to safely remove larger size particles. Supplier costs for larger diameter (greater than 65 μm) powders are usually lower than for smaller diameter (less than 50 μm) powder size distributions.

In the kinetic spray process, there are no high particle or substrate temperatures to produce coatings resulting in; little or no oxide formation in the coatings and no melting or thermal softening of the particles. Previous studies[1,6] have shown that the oxide content in the coatings is comparable to the oxide content in the starting powders. This low temperature coating procedure also limits the reactivity of the individual material components of the starting powders resulting in little to no phase changes compared with the subsequent coatings material phases. Reactivity with air is also minimized. The Ta particles, during the coating formation, never reach temperatures approaching 500 °C, curtailing any reactivity and providing one with the ability to produce coatings in ambient air using He or air as the main gas.

The lack of melting produces little thermal stress (from the phase change from liquid to solid) in the coating unlike thermal spray coatings. The cold working (peening) and compressive stress (from the high velocity impacting particles) allows one to produce extremely thick coatings using the kinetic spray method. Indeed there really is no coating thickness limitation. We have produced coatings several centimeters thick without delamination or other effects commonly seen with thermal spray coatings.

3. Experimental

Refer to Fig. 1. Nitrogen gas pressure was held constant at 2.4 MPa (350 psi) for the powder feeder and 2.0 MPa (300 psi) when air was used as the main gas flow, and 1.7 MPa (250 psi) for the powder feeder and 1.37 MPa (200 psi) when He was used as the main gas flow. Temperatures of the main gas ranged from 204 to 427 °C, which provided a corresponding range of the particle velocities. He provides substantially higher gas velocities with correspondingly higher particle velocities (Eq 1 and Ref 1,6,13,17-19).

Two types of converging-diverging supersonic gun nozzles were used in this study. The first (designated nozzle A) has a rectangular exit aperture of approximately 2 × 10 mm with a throat of approximate diameter 2.8 mm, 80 mm length (throat to nozzle exit), and an entrance cone whose diameter decreased from 7.5 mm to the 2.8 mm throat region.

The second nozzle configuration used (designated nozzle B)

has a rectangular exit aperture of approximately 5 × 12.5 mm with a throat of approximate diameter of 2.8 mm, 278 mm length (throat to nozzle exit), and an entrance cone whose diameter decreased from 7.5 mm to the 2.8 mm throat region. The primary differences between nozzles A and B are the nozzle length after the throat region, exit area, and the expansion profiles in the diverging section of the nozzles.

Stand-off distance from the end of both nozzles to the substrate was 20 mm with a powder feed rate of approximately 1 g/s. The traverse rate of the substrate pass the exit of both nozzles was 2.54 mm/s. All of the brass substrates were sandblasted to roughen the surface and improve adhesion of the coatings and sprayed in one pass.

Ta powders, received from F.J. Brodmann (Harvey, LA), are shown in the scanning electron microscope (SEM) photos in Fig. 2(a)-2(b) and in Fig. 3(a)-3(b) (etched optical micrographs). The powders were produced by the reduction of $K_2(TaF_7)$ with sodium metal using the following reaction:

$$K_2(TaF_7) + 5\,Na = 5NaF + 2\,KF + Ta \qquad \text{(Eq 2)}$$

and have a measured size distribution shown in Fig. 4, where $D(10) = 69$ μm, $D(50) = 79$ μm, and $D(90) = 118$ μm, where $D(X)$ is the diameter at which X vol% have a smaller diameter (measured with a Malvern Mastersizer). The powders have a sponge-like open cell appearance. A polished and etched cross section of the Ta powder is shown in Fig. 3(a)-(b). One can clearly distinguish the different grain boundaries and sponge-like surface morphology of the powders in Fig. 2(a)-(b).

Calculated main gas velocities at the nozzle exit can be found in Fig. 5. The particle velocities were calculated from one-dimensional modeling using analytical equations based on inlet

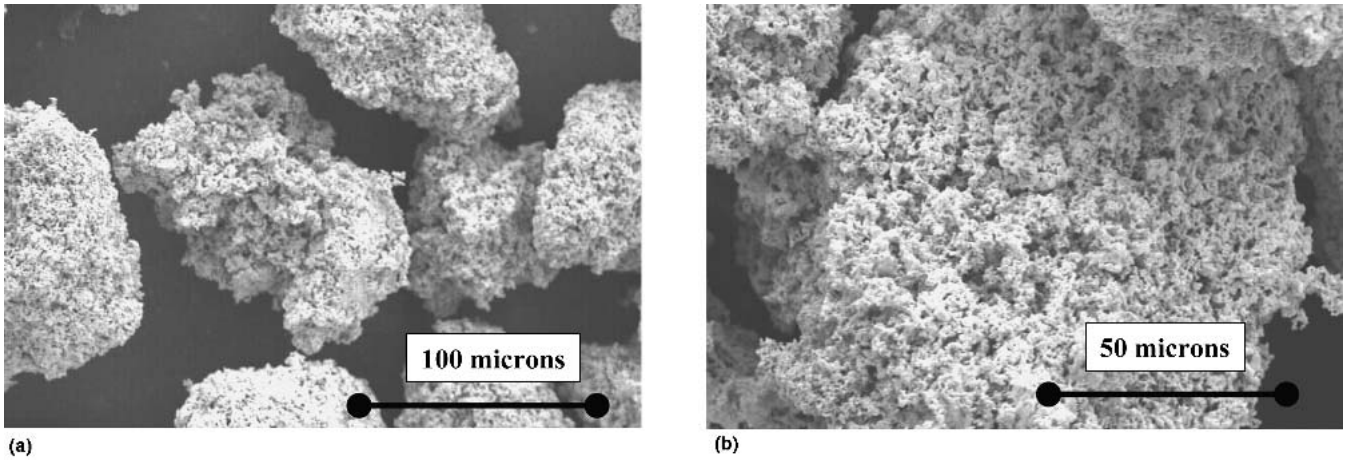

Fig. 2 SEM photos **(a)** 500× and **(b)** 1000× of Ta powder used in coatings

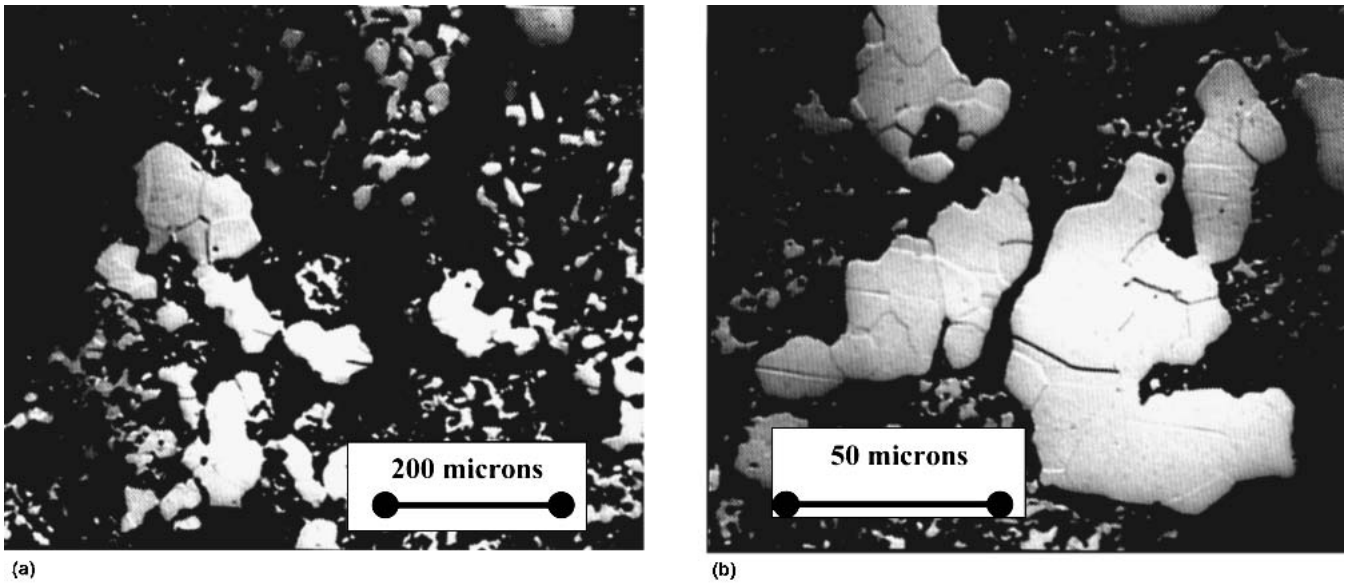

Fig. 3 **(a)** Etched optical micrographs, **(b)** higher magnification of Ta powder showing internal grain boundaries

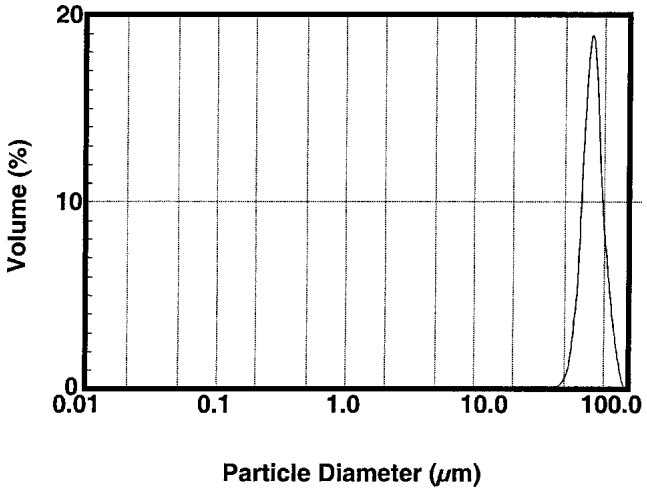

Fig. 4 Particle size distribution of Ta powder as function of volume percent: $D(10) = 69$ μm, $D(50) = 79$ μm, and $D(90) = 18$ μm

gas conditions and nozzle area versus length and assuming isentropic (adiabatic and frictionless) gas flows. Theoretical particle velocities for a 76 μm diameter Ta particle are calculated from the drag forces and are shown in Fig. 6 for both air and He (main gases) as a function of main gas temperature for both nozzles. Previous studies[1,6,13,17-19] have demonstrated excellent agreement between calculated particle velocity values and actual measured particle velocities (for spherical particles). Higher gas velocities for all main gas temperatures are generated using nozzle B (Fig. 5) compared with nozzle A, with corresponding higher particle velocities (Fig. 6). Particle velocity is also proportional to the square root of the distance traveled in the nozzle,[17] therefore nozzle B should give higher particle velocities than Nozzle A all other parameters equal. Using He as the main gas increases the particle velocity by a factor of 2 or better. One would expect a higher degree of plastic deformation, void reduction, and peening effects (cold working) to incur with the Ta particles sprayed using nozzle B (287 mm throat to exit length) and He as the main gas.

Experimental coatings, at constant powder feed rate (approximately 1 g/s) using one pass in front of the nozzle exit, were used to determine the relative deposition efficiency of the Ta coatings (i.e., thickness) for each different spraying condition tested. Hardness (degree of work hardening), adhesion (degree of bonding), and porosity (degree of void reduction) measurements are compared with the microstructure of the coatings to determine what affect the particle's velocity had on the degree of plastic deformation occurring in the coatings.

4. Results

Table 1 contains the coating thickness variation as a function of main gas temperature, main gas type, and nozzle type for one pass across the nozzle exit. From the table, one observes that increasing coating thickness (increased deposition efficiency for a 1 g/s powder feed rate) is demonstrated with increasing main gas temperature or the use of He as the main gas (i.e., increasing particle velocity) for both nozzle A or nozzle B. Nozzle B had a

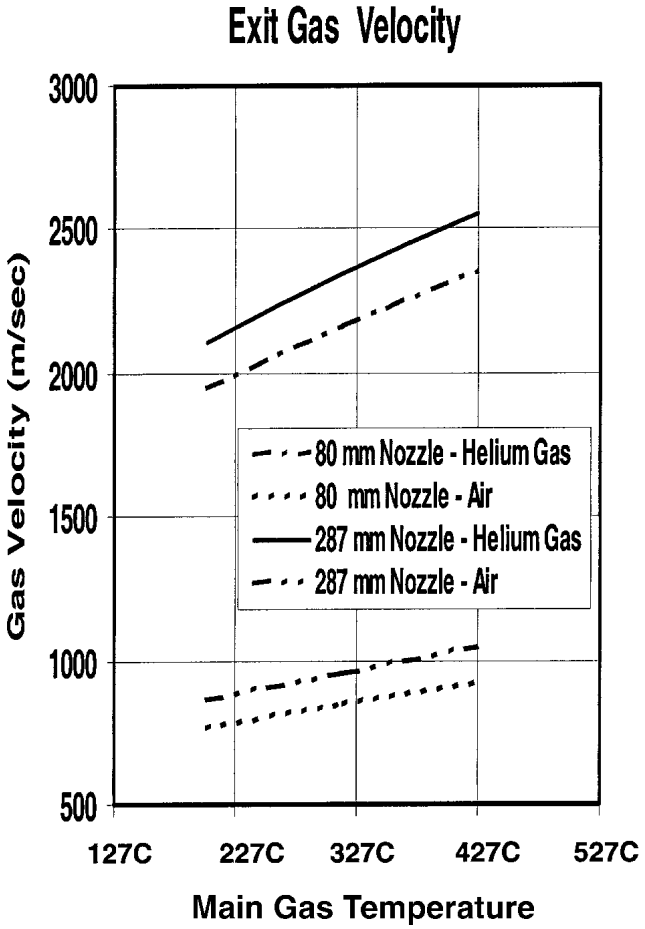

Fig. 5 Theoretical calculations (one dimensional) of exiting gas velocity for nozzle A (80 mm nozzle length) and B (287 mm nozzle length)as function of main gas temperature

maximum coating thickness of 2.22 mm at a main gas temperature of 427 °C. Nozzle A measured a maximum coating thickness of 2.1 mm at main gas temperature of 427 °C.

Below 204 °C main gas temperature, no coatings were produced. Presumably, for this particle size distribution we are below the mean critical particle velocity-needed for coating formation.[1,6] However, there is evidence that particle temperature may also have a critical influence on coating formation, with some evidence for a threshold particle temperature. No coatings were formed for He $T < 204$ °C, nozzle B, however using nozzle A, Air $T = 427$ °C, coatings were produced. From Fig. 6 the calculated particle velocities using nozzle B at the lower main gas temperature 204 °C should still have been higher than the particles using nozzle A with air $T = 427$ °C. The fact that coatings could be produced at lower particle velocities suggests that the combination of particle velocity and particle temperature may be an important parameter in the coating formation. Thicker coatings were measured when nozzle B was used compared with nozzle A using similar spraying parameters, consistent with the predicted higher velocities for nozzle B (Fig. 5 and 6). Coating thickness, when air was used as the main gas, was substantially reduced compared with the coatings produced when He was used as the main gas.

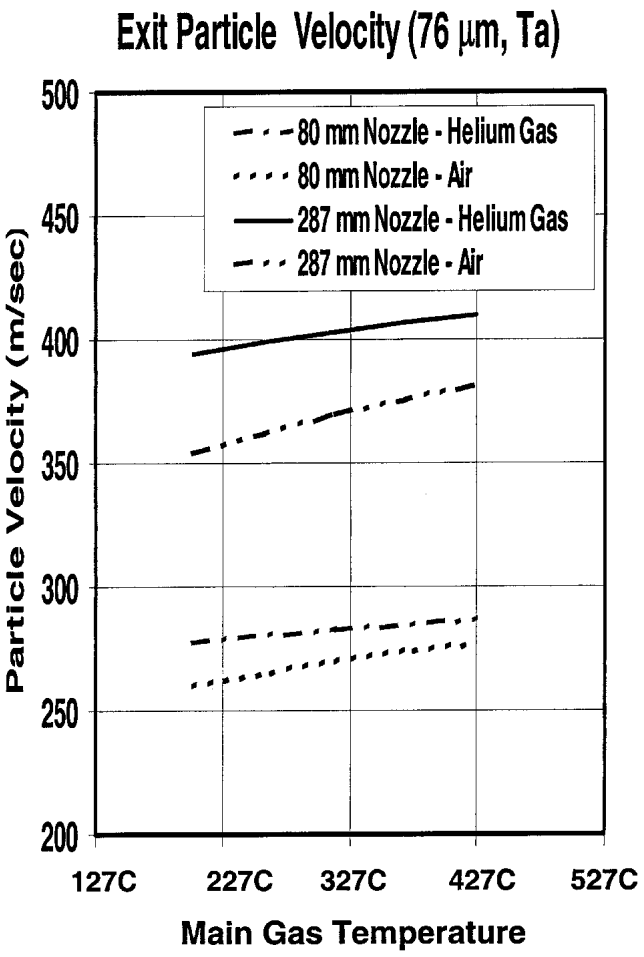

Fig. 6 Theoretical particle velocities for a 76 μm diameter Ta particle are calculated from the drag forces for both air and He (main gases) as a function of main gas temperature for nozzle A (80 mm nozzle length) and B (287 mm nozzle length)

Table 1 Coating Thickness as Function of Nozzle, Main Gas Type, and Main Gas Temperature

Main Gas Temperature, °C	Main Gas	Nozzle	Maximum Coating Thickness, mm, at 1 g/s Feed Rate
204	Helium	B	1.68
315	Helium	B	1.96
427	Helium	B	2.22
315	Helium	A	1.9
427	Helium	A	2.1
427	Air	A	1.36

Table 2 contains the hardness values measured for the initial starting powder and bulk Ta. Hardness values were measured using a Matsuzawa Model MXT70-UL (Tokyo, Japan) ultra microhardness tester. The initial powder had a measured hardness of 155.5 HVat 0.1 g load, roughly halfway between reported values for bulk Ta in the cold worked (200 HV[2]) and the annealed (90-100 HV[2]) states.

Table 3 contains the hardness values measured for coatings produced using the spray parameters shown. Although the hardness differences between the coatings is relatively small (keeping the same nozzle, main gas, and varying only main gas temperature), there is definitely a trend, and the small differences in hardness when one varies the main gas temperature may be the result of Ta ability to respond slowly to cold working or a function of the particle's temperature (temperature dependence of yield strength). In all cases, when He is used for the main gas, we measure an increase in the hardness of the coatings compared with the starting powder.

Table 2 Hardness Measurements for Bulk Tantalum and Starting Powder

Material	Hardness HV
Starting powder	155.5
Bulk (cold worked)	200
Bulk (annealed)	100

Table 3 Hardness Measurements for Kinetically Sprayed Tantalum Coatings

Main Gas Temperature, °C	Main Gas	Nozzle	Hardness HV at 5 g Load
204	Helium	B	184.9
315	Helium	B	171.8
427	Helium	B	176.2
315	Helium	A	166.8
427	Helium	A	164.5
427	Air	A	135.6

Table 4 Porosity Measurements for Kinetically Sprayed Tantalum Coatings

Main Gas Temperature, °C	Main Gas	Nozzle	Porosity, %
204	Helium	B	3.15
315	Helium	B	3.28
427	Helium	B	4.07
427	Air	A	16.31
315	Helium	A	9.6
427	Helium	A	8.77

Presumably, this is a direct result of the plastic deformation and the peening effect caused by incoming particles[1,6] impacting on the previously deposited coating producing a work hardening effect. We also observe an increase in the hardness values for the coatings produced with nozzle B compared with nozzle A coatings. The highest hardness value, interestingly enough, occurs for the coating produced with nozzle B, He main gas and a temperature of 204 °C.

Where air was used as the main gas, the coating hardness, actually decreased in hardness compared with the starting powder. The porosity for these coatings was also the highest (16.31% compared with 9% for the other coatings same main gas and nozzle) and the adhesion was the lowest of the coatings. Table 4 shows that nozzle A coatings also have higher porosity than nozzle B coatings suggesting that the lower particle velocities of

nozzle A may allow for insufficient void reduction (i.e., increased porosity), which could contribute to an artificially lower measured hardness.

Porosity measurements for the Ta coatings were measured using a He pycnometer (Micrometrics AccuPyc 1330) and are shown in Table 4. Samples were initially measured, then the sample was sealed using an anaerobic sealant (Loctite 990) and the volume was measured again to determine open pore volume.

Looking at Table 4, we observe that higher porosity occurs for the sample coatings produced using nozzle A, with the highest porosity of all measured when air was used as the main gas in nozzle A. The Ta particles for this coating have the lowest velocity since air was used for the main gas.

One could assume that the lower particle velocity translates into a reduction in the particle's kinetic energy with subsequently reduced plastic deformation and void reduction,[1,6] resulting in increased porosity. A similar trend (decreasing particle velocity resulting in increased porosity) is observed among the coatings produced using the nozzle A with He as the main gas compared with the coatings produced using nozzle B with He main gas. Nozzle B, which has higher particle and gas velocities compared with nozzle A (Fig. 5-6), produced lower measured coating porosity than coatings produced with nozzle A. Little change was observed in the coating porosity when using nozzle B and He main gas as a function of main gas temperature suggesting an upper limit of approximately 1% for the accuracy of the instrument and porosity measurement technique for these coatings.

Nozzle B is accelerating the particles at sufficient velocity at main gas temperatures as low as 204 °C to provide for a high degree of plastic deformation and void reduction at impact producing low porosity coatings. We will return to this discussion when we look at the micrographs for each of the coatings.

Adhesion measurements between the coating and the substrate were attempted using a South Bay Technologies Model 360 rotary disk cutter to core a 2.97 mm diameter island (using a silicon carbide slurry) through the Ta coating to the substrate. An adhesive pull stud (2.69 mm diameter) would then be epoxy bonded to this island for pull testing. The Ta coring required in excess of 24 h to break through to the substrate and resulted in physical damage to the coating with subsequent delamination of the island in most cases. We abandoned this procedure and directly bonded the pull studs to the coating for testing.

While this method will not provide a quantitative number, we should be able to get a relative number for how strong the particle-particle adhesion is for the coatings produced at the different spray conditions tested. A series of four measurements were taken and the average results are displayed in Table 5.

Table 5 lists the adhesion testing results for the coatings sprayed using the conditions listed above. Again note that nozzle B coatings (higher particle velocities) outperform the coatings produced using nozzle A (lower particle velocities). The coating sprayed at 427 °C with He and nozzle A produced an adhesion measurement approaching the coatings produced with nozzle B. The lowest adhesion measurement was produced from the coatings produced using air as the main gas (lowest particle velocity). Interestingly enough, we observe that the failure mechanism for the nozzle A coatings were cohesive, while the failure mechanism for nozzle B produced coatings were in the epoxy regardless of the spray conditions tested. This is consistent with higher particle velocities of nozzle B demonstrating lower porosities, higher adhesion strengths, and higher hardnesses.

Table 5 Adhesion Measurements for Kinetically Sprayed Tantalum Coatings

Main Gas Temperature, °C	Main Gas	Nozzle	Adhesion Strength, kpsi	Failure Mode
204	Helium	B	11.4	Epoxy
315	Helium	B	10.8	Epoxy
427	Helium	B	10.9	Epoxy
427	Air	A	3.8	Cohesive
315	Helium	A	7.4	Cohesive
427	Helium	A	9.06	Cohesive

5. Discussion

Figure 7(a) is a SEM photo for an etched coating produced at a main gas temperature (He) of 204 °C using nozzle B. Figure

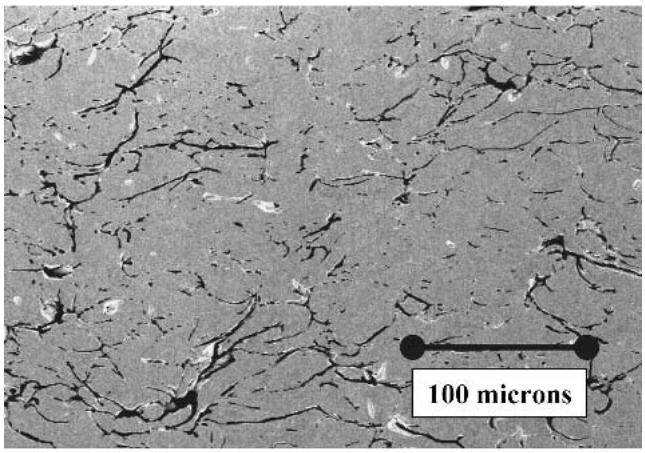

(a)

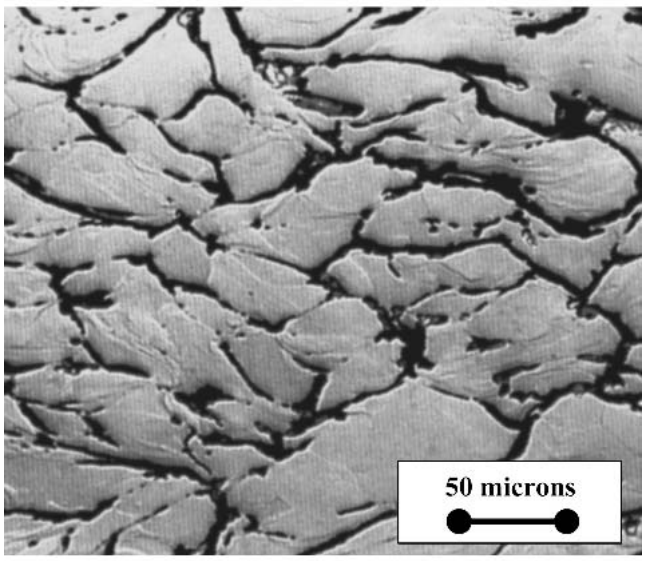

(b)

Fig. 7 SEM photo **(a)** at a magnification of 400×, **(b)** etched optical photo at magnification of 1000× of coatings sprayed at 204 °C, with He (main gas) and with nozzle B

7(b) is an optical micrographs of the same coating heavily etched to reveal the internal grain structures. Figures 7(a) and (b) reveals a dense coating structure where the initial sponge-like morphology of the particles has been transformed thru plastic deformation into a dense solid particle structure. One can easily see in Fig. 7(b) that the internal grain boundaries have plastically deformed and tend to conform with the deformed shapes of the particles (see etched outer surfaces outlining the original particles in Fig. 7b, 8b, 9b, and 10b).

As the main gas temperature is increased further to 427 °C (particle velocity and particle temperature also increasing), we observe (Fig. 8b and 9b) regions where it is difficult to distinguish between the original particles boundaries. Figure 8(b) shows the high degree of internal plastic deformation that the particles have under gone. The internal grain boundaries of the starting powders have orientated anisotropically, with particles flattening parallel to the coating surface.

Figure 9(a) is an SEM photo of an etched coating produced at 427 °C, with He as the main gas, and with nozzle A. Etched optical micrographs of this coating are shown in Fig. 9(b). Comparisons between Fig. 9(b) and 8(b) clearly show a reduced degree of plastic deformation, less flattening of the particles, and higher porosity. This is also shown in Tables 3, 4, and 5. The sample coatings produced using nozzle A have higher porosity, lower adhesion, and lower hardness (work hardening)

Figure 10(a) is a SEM photo of a coating produced at 427 °C, using air as the main gas, and again nozzle A. We can immediately observe the effect that the lower particle velocity has on the coatings. Very little plastic deformation has occurred as shown in the figures. The original particle shape has survived relatively intact. The particles have consolidated from the origi-

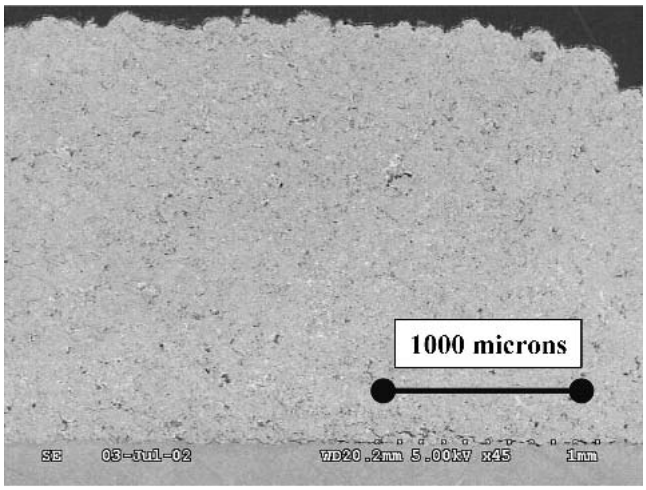

(a)

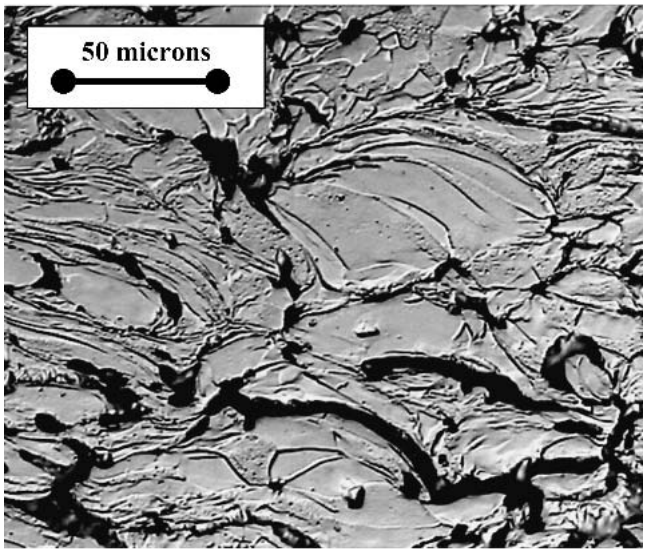

(b)

Fig. 8 **(a)** SEM photo at a magnification of 45×; **(b)** etched optical photo at a magnification of 1000× of coatings sprayed at 427 °C, with He (main gas) and with nozzle B. Note the degree of internal grain deformation.

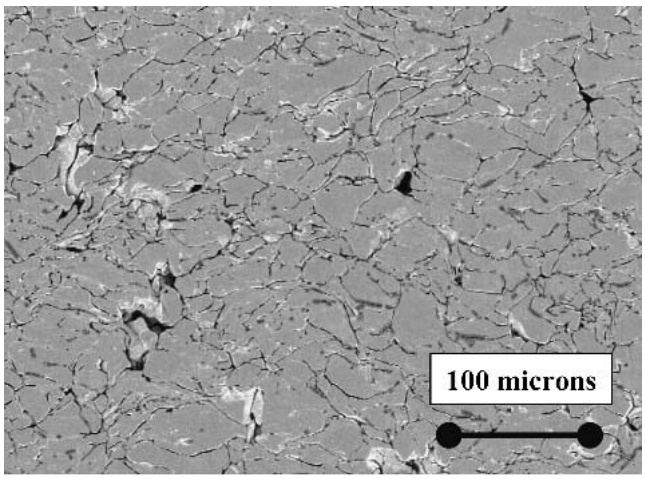

(a)

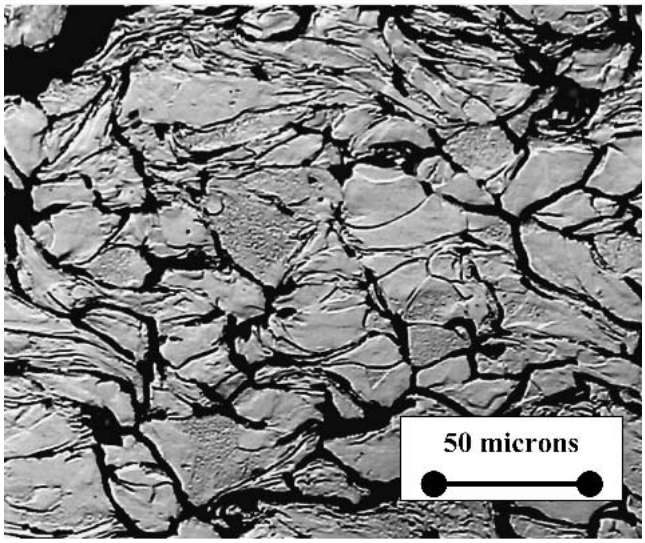

(b)

Fig. 9 **(a)** SEM photo at a magnification of 300×; **(b)** etched optical photo at a magnification of 1000× of coatings sprayed at 427 °C, with He (main gas) and with nozzle A. Note the degree of internal grain deformation.

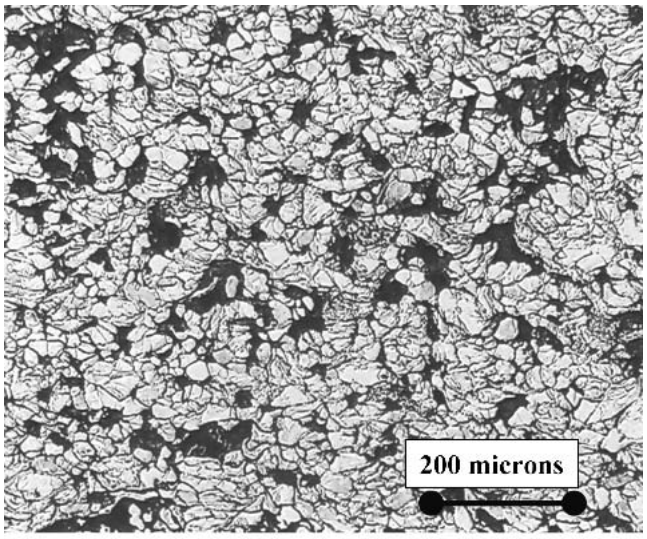

(a)

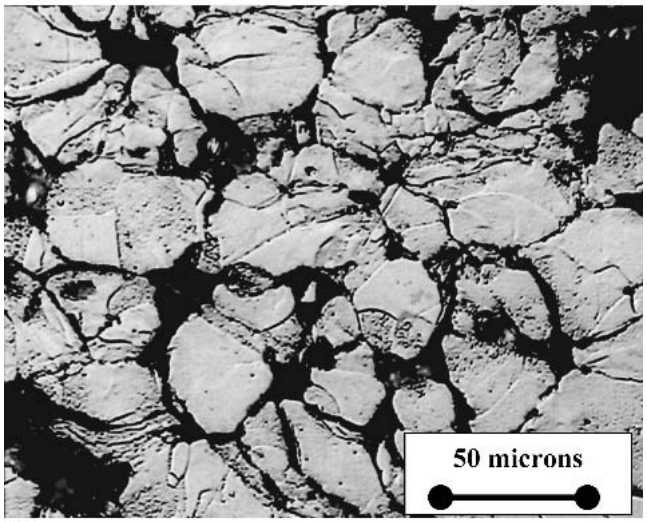

(b)

Fig. 10 Etched optical photos: **(a)** at a magnification of (200×), **(b)** at a magnification of (1000×) of coating sprayed at 427 °C (800 °F), air (main gas) and nozzle A. Note the degree of internal grain deformation compared with Fig. 8(b) and 9(b).

nal spongy-like structure (Fig. 2 and 3), however little deformation is observed in the internal grain boundaries, (Fig. 10b), resulting in a reduction in particle-particle bonding. This is demonstrated in the low hardness, high porosity, and low adhesion of the coating measured in Tables 3, 4, and 5. The hardness of the particles actually decreased from the original powder values measured.

6. Summary

We demonstrated that thick Ta coatings can be produced in air with excellent adhesion, low porosity, and increased hardness. Analysis of the Ta coatings reveals plastic deformation and internal grain reorientation similar to that observed with the aluminum (Al) particle testing previously reported.[1,6] The Al particle study shows that increasing the main gas temperature and particle temperature resulted in increased hardness, decreasing porosity, and increased adhesion as did the Ta coatings. Interestingly, the mechanical properties of the annealed bulk Ta (melting point 2996 °C, density 16.65g/cm^3, hardness 90 HV, ultimate tensile strength 650 MPa, elastic modulus 186 GPa, shear modulus 69 GPa) are significantly higher that the mechanical properties of Al (melting point 650 °C, density 2.7g/cm^3, hardness 15 HV, ultimate tensile strength 45-70 MPa, elastic modulus 69 GPa, shear modulus 25 GPa.),[2] yet both materials produce coatings at roughly the same particle velocity. Ta has a shear modulus of 69 GPa and elastic modulus 186 GPa, while Al has a shear modulus is 25 GPa and elastic modulus 69 GPa. The calculated velocity for a Ta particle (76 μm diameter and main gas temperature 371 °C) is approximately 410 m/s (see Fig. 6). The calculated velocity for an Al particle (85 μm diameter and main gas temperature 371 °C) is 450 m/s.[1] Since the kinetic energy for both particles is roughly the same the shear and elastic modulus may be the dominating factor in the plastic deformation and coating formation for the Ta and Al. It should also be noted that the shear and elastic modulus are both temperature dependent. The particle temperature could also be playing a critical role in the formation of these coatings. Subsequent experiments using tungsten powders (elastic modulus 406 GPa) were not able to produced coatings using our experimental apparatus. Presumably, there is insufficient particle velocity and temperature (lower kinetic energy) for the plastic deformation of the tungsten particles (i.e., particles are below the mean critical velocity needed for coating formation[1,6,13-19]).

The kinetic spray process has also demonstrated that Ta coatings can be produced, in air, without reaction from the atmosphere. No inert gas shielding or vacuum conditions were required as in other coating methods.[3-5]

Improved coatings were produced when He was used as the main gas as compared with air. The longer nozzle B coatings demonstrated increased adhesion, lower porosity and higher work hardening compared with coatings produced with shorter nozzle A. In the micrographs of the Ta coatings increased plastic deformation of the particles and internal grain structure is observed (flattening of the particles and the disappearance of some of the original particle boundaries) for nozzle B coatings. Any change in the spray parameters, which correspondingly leads to increasing the particle velocity, increases the degree of plastic deformation observed in the coatings providing there is sufficient kinetic energy to over come the yield strength of the particles. It is this increased degree of plastic deformation that leads to void reduction, increased hardness, adhesion, and decreased porosity. Higher particle velocities improve the material properties of the coatings resulting in a high degree of plastic deformation and particle-particle bonding of the coatings and provide excellent agreement with the results from previous study using Al particles.[1]

Acknowledgments

The authors would like to thank Nilesh Patel for the porosity and adhesion testing and Donna Hurlock for the optical micrographs and hardness data. We thank Dr. Taeyoung Haun for the gas and particle velocities calculations. We also acknowledge

discussion and helpful suggestions of Dr. John R. Smith, Dr. Alaa Elmoursi, Dr. Rich Teets, and Dr. Zhibo Zhao.

References

1. T.H. Van Steenkiste, J.R. Smith, and R.E. Teets: "Aluminum Coatings Via Kinetic Spray With Relatively Large Powder Particles," *Surf. Coat. Technol.*, 2002, *154,* pp. 237-52.
2. Anon., *ASM Metals Handbook,* Vol. 2, *Properties and Selection: Nonferrous Alloys and Special-Purpose Materials,* ASM International, Materials Park, OH, 1990.
3. T. Kinos, S.L. Chen, P. Siitonen, P. Kettunen: "Densification of Plasma-Sprayed Titanium and Tantalum Coatings," *J. Therm. Spray Technol.*, 1996, *4,* pp. 439-44.
4. S.L. Lee, M. Cipollo, D. Windover, and C. Rickard: "Analysis of Magnetron-Sputtered Tantalum Coatings versus Electrochemically Deposited Tantalum from Molten Salt," *Surf. Coat. Technol.* 1999, *120-121,* pp. 44-52.
5. C. Hayes, J.L. Watson, and J.P. Walker: "Tantalum Coatings for the Petrochemical Industry" in *Thermal. Spray Science and Technology*, C.C. Berndt and S. Sampath, ed., ASM International, Materials Park, OH, 1995, pp. 589-93.
6. T.H. Van Steenkiste, J.R. Smith, R.E. Teets, J.J. Moleski, D.W. Gorkiewicz, R.P. Tison, D.R. Marantz, K.A. Kowalsky, W.L. Riggs, P.H. Zajchowski, B. Pilsner, R.C. McCune, and K.J. Barnett: "Kinetic Spray Coatings," *Surf. Coat. Technol.,* 1999, *111,* pp. 62-71.
7. T.H. Van Steenkiste, J.R. Smith, R.E. Teets, J.J. Moleski, and D.W. Gorkiewicz, U.S. Patent 6 139 913, Kinetic Spray Coating Method and Apparatus (Oct. 31, 2000)
8. J.R. Smith, T.H. Van Steenkiste, and W.J. Meng, U.S. Patent 6 189 663, Spray Coatings for Suspension Damper Rods (Feb. 20, 2001).
9. G.H. Smith, N.Y. Kenmore, R.C. Eschenbach, and J.F. Pelton, U.S. Patent 2 861 900, Jet Plating of High Melting Point Materials (Nov. 25, 1958).
10. C.F. Rocheville, U.S. Patent 3 100 724, Device for Treating the Surface of a Workpiece (Aug. 13, 1963).
11. J.A. Browning: "What If We're Right?" in *Thermal Spray: A United Forum for Scientific and Technological Advances*, C.C. Berndt ed., ASM International, Materials Park, OH, 1997, pp. 15-18.
12. J.A. Browning, U.S. Patent 5 271 96, Thermal Spray Method Utilizing In-Transit Powder Particle Temperatures Below Their Melting Point (Dec. 21, 1993).
13. A.P. Alkimov, V.F. Kosarev, A.N. Papyrin: "A Method of Cold Gas-Dynamic Deposition," *Dokl. Akad. Nauk,SSSR,*, 1062, *318,* 1990.
14. A.P. Alkhimov, A.N. Papyrin, V.F. Kosarev, N.I. Nesterovich, and M.M. Shushpanov, U.S. Patent 5 302 414, Gas Dynamic Spraying Method for Appling a Coating (April 12, 1994).
15. R.C. McCune, A.N. Papyrin, J.N. Hall, W.L. Riggs II, and P.H. Zajchowski: "An Exploration of the Cold Gas-Dynamic Spray Method for Several Materials Systems" in *Thermal Spray Science & Technology,* C.C. Berndt and S. Sampath, ed., ASM International, Materials Park, OH, 1995, pp. 1-5.
16. R.C. McCune, W.T. Donlon, E.L. Cartwright, A.N. Papyrin, E.F.Rybicki, and J.R. Shadley: "Characterization of Copper and Steel Coatings Made by the Cold Gas-Dynamic Spray Method" *Thermal Spray: Practical Solutions for Engineering Problems*, C.C. Berndt, ed., ASM International, Materials Park, OH,1996, pp. 397-403.
17. R.C. Dykhuizen and M.F. Smith: "Gas Dynamic Principles of Cold Spray," *J. Therm. Spray Technol.,* 1998, *7,* pp. 205-12.
18. M.F. Smith, J.E. Brockmann, R.C. Dykhuizen, D.L. Gilmore, R.A. Neiser, and T.J. Romer: "Cold Spray Direct Fabrication–High Rate, Solid State, Material Consolidation," in *Freeform, and Additive Fabrication,* D. Dimos, S.C. Danforth, and M. Cima, ed., Materials Research Society, Warrendale, PA, 1999, pp. 65-76.
19. R.C. Dykhuizen, M.F. Smith, D.L. Gilmore, R.A. Neiser, X. Jiang, and S. Sampath: "Impact of High Velocity Cold Spray Particles," *J. Therm. Spray Technol.*, 1999, *8,* p. 559.
20. D.L. Gilmore, R.C. Dykhuizen, R.A. Neiser, T.J. Roemer, and M.F. Smith: "Particle Velocity and Deposition Efficiency in the Cold Spray Process," *J. Therm. Spray Technol.,* 1999, *8,* p. 576.
21. M. Jacobson, A.R. Cooper, and J. Nagy, Explosibility of Metal Powders U.S. Bureau of Mines, Washington, DC, RI 5624, 1960.